Available at www.sciencedirect.com

ScienceDirect

journal homepage: www.elsevier.com/locate/watres

Coupled factors influencing the transport and retention of *Cryptosporidium parvum* oocysts in saturated porous media

Hyunjung N. Kim [a], *Sharon L. Walker* [a], *Scott A. Bradford* [b,*]

[a] *Department of Chemical and Environmental Engineering, University of California, Riverside, CA 92521, USA*
[b] *USDA, ARS, US Salinity Laboratory, Riverside, CA 92507, USA*

ARTICLE INFO

Article history:
Received 9 June 2009
Received in revised form
11 September 2009
Accepted 17 September 2009
Available online 22 September 2009

Keywords:
Pathogen
Transport
Cryptosporidium parvum oocysts
Hydrodynamic force
Pore structure
Steric repulsion

ABSTRACT

The coupled role of solution ionic strength (IS), hydrodynamic force, and pore structure on the transport and retention of viable *Cryptosporidium parvum* oocyst was investigated via batch, packed-bed column, and micromodel systems. The experiments were conducted over a wide range of IS (0.1–100 mM), at two Darcy velocities (0.2 and 0.5 cm/min), and in two sands (median diameters of 275 and 710 μm). Overall, the results suggested that oocyst retention was a complex process that was very sensitive to the solution IS, the Darcy velocity, and the grain size. Increasing IS led to enhanced retention of oocysts in the column, which is qualitatively consistent with predictions of Derjaguin–Landau–Verwey–Overbeek theory. Conversely, increasing velocity and grain size resulted in less retention of oocysts in the column due to the difference in the fluid drag force and the rates of mass transfer from the liquid to the solid phase and from high to low velocity regions. Oocyst retention was controlled by a combined role of low velocity regions, weak attractive interactions, and/or steric repulsion. The contribution of each mechanism highly depended on the solution IS. In particular, micromodel observations indicated that enhanced oocyst retention occurred in low velocity regions near grain–grain contacts under highly unfavorable conditions (IS = 0.1 mM). Oocyst retention was also found to be influenced by weak attractive interactions (induced by the secondary energy minimum, surface roughness, and/or nanoscale chemical heterogeneity) when the IS = 1 mM. Reversible retention of oocysts to the sand in batch and column studies under favorable attachment conditions (IS = 100 mM) was attributed to steric repulsion between the oocysts and the sand surface due to the presence of oocyst surface macromolecules. Comparison of experimental observations and theoretical predictions from classic filtration theory further supported the presence of this weak interaction due to steric repulsion.

Published by Elsevier Ltd.

1. Introduction

Cryptosporidium parvum (*C. parvum*) is a fecal borne protozoan parasite that can cause gastrointestinal illness in humans, cattle, and wildlife (Bitton, 2005). A common waterborne disease caused by *C. parvum* is known to be cryptosporidiosis, which can result in serious diarrhea and can be fatal for people with a compromised immune system (Centers for Disease Control and Prevention, 1997). *C. parvum* is considered to be one of the most problematic waterborne pathogens in developed countries because it is resistant to all practical levels of chlorination, surviving for 24 h at 1000 mg/L of free chlorine (Brush et al., 1998; Darnault et al., 2004) and it has a relatively small infectious dose (as few as 10 oocysts) in comparison to other

* *Corresponding author*. Tel.: +1 951 369 4857; fax: +1 951 342 4964.
E-mail address: Scott.Bradford@ars.usda.gov (S.A. Bradford).
0043-1354/$ – see front matter Published by Elsevier Ltd.
doi:10.1016/j.watres.2009.09.041

pathogens (Bitton, 2005). Hence, much attention has been paid by water utilities to efficiently remove this pathogen during drinking water purification and in filtration units (e.g., river-bank filtration, deep-bed filtration, and slow sand filtration) (Timms et al., 1995; Huck et al., 2002; Tufenkji et al., 2002). In order to maximize the removal efficiency of oocysts from source water, the fundamental mechanisms controlling the transport and retention behavior of *C. parvum* oocysts in porous media need to be well understood. Several obstacles exist to achieving this goal, including: the diversity of oocysts' species, difficulty in quantification, and toxicity to humans.

Considerable research has investigated mechanisms of oocysts deposition onto and interaction with solid surfaces in radial stagnation point flow (RSPF) systems (e.g., Kuznar and Elimelech, 2004, 2005, 2006; Liu et al., 2009), packed-bed columns (e.g., Harter et al., 2000; Hsu et al., 2001; Tufenkji et al., 2004; Bradford and Bettahar, 2005; Tufenkji and Elimelech, 2005b; Cortis et al., 2006), and with atomic force microscopy (e.g., Considine et al., 2001; Byrd and Walz, 2007). Factors that have been found to contribute to oocyst deposition and interaction mechanisms include: solution chemistry (i.e., ionic strength (IS), ion valence, and pH), velocity, and grain size/shape. Most studies reported that physicochemical interactions dominantly controlled oocyst deposition (e.g., Harter et al., 2000; Hsu et al., 2001; Tufenkji et al., 2004; Tufenkji and Elimelech, 2005b). However, recent studies have also emphasized the importance of low velocity regions on oocyst retention in a packed-bed column (Tufenkji et al., 2004; Bradford and Bettahar, 2005). This implies that studies investigating the coupled role of these factors (e.g., IS, velocity, grain size, pore size distribution, etc.) on oocyst deposition in porous media are required to better understand removal mechanisms of oocysts in porous media, but currently relevant studies are scarce. Several studies have reported the importance of this coupled role on the deposition of colloids and bacteria to solid surfaces (Bradford et al., 2007; Torkzaban et al., 2007, 2008). For example, experimental and theoretical results indicated that particle retention was very sensitive to hydrodynamic force, especially when the particles were weakly associated with solid surfaces (i.e., secondary energy minimum interaction). Since the size of oocysts is relatively large (ca. 4–6 μm) compared to other bacterial/viral pathogens (≤ 2 μm), it is expected that the oocysts may experience an even greater impact from hydrodynamic force (Torkzaban et al., 2007).

Many studies have recently demonstrated that classic colloid filtration theory (CFT) (Yao et al., 1971) is often inaccurate for describing (bio)colloid transport under unfavorable (Bradford et al., 2002; Hahn and O'Melia, 2004; Li et al., 2006; Tufenkji and Elimelech, 2005a, b) and favorable (Cortis et al., 2006; Torkzaban et al., 2008; Haznedaroglu et al., 2009; Kim et al., 2009a) conditions predicted by classic Derjaguin–Landau–Verwey–Overbeek (DLVO) theory (Derjarguin and Landau, 1941; Verwey and Overbeek, 1948). Note that below the terms "unfavorable" and "favorable" are based on the DLVO prediction. Under unfavorable conditions deviations from CFT predictions have been attributed to lack of consideration of pore structure and surface roughness, fluid drag forces, colloid–colloid interactions, secondary minimum interaction, and/or chemical heterogeneity. Under favorable conditions deviations may also occur due to steric repulsion induced by macromolecules on the surface of microbes. Oocysts are also thought to possess glycoproteins in the inside and outside of their wall (Harris and Petry, 1999). Close inspection of the literature reveals the presence of weak, reversible interactions for oocysts under conditions that DLVO theory predicts as chemically favorable and that should result in irreversible oocyst deposition (Cortis et al., 2006; Kuznar and Elimelech, 2006; Liu et al., 2009). For instance, studies conducted by Kuznar and Elimelech (2006) and Liu et al. (2009) clearly demonstrated that the presence of macromolecules on oocyst surfaces hindered the deposition of oocysts to a quartz surface in RSPF studies. Cortis et al. (2006) observed significant oocyst breakthrough and the gradual release of oocysts from columns as a function of time even under chemically favorable conditions (i.e., IS = 100 mM). In addition, they observed a significant decrease in oocyst removal efficiency with IS when IS ≥ 3 mM. This observation indicates that steric repulsion may be an important mechanism in oocyst retention as suggested by the recent review (Tufenkji et al., 2006). However, no systematic column studies have yet been reported using *Cryptosporidium* oocysts from this point of view.

This study was designed to investigate the coupled role of IS and hydrodynamic force (Darcy velocity and grain size) on the fate and transport of *Cryptosporidium parvum* oocysts in saturated porous media. For this purpose, a range of solution IS (0.1–100 mM), Darcy velocities (0.2 and 0.5 cm/min), and sand grain sizes (median diameter of 275 and 710 μm) were applied in transport experiments. Findings from this study demonstrated the importance of low velocity regions and pore structure in oocyst retention under unfavorable conditions, and reversible oocyst retention by steric repulsion under favorable conditions.

2. Materials and methods

2.1. *Cryptosporidium parvum* oocyst selection and solution chemistry

Viable oocysts were obtained from the Sterling Parasitology Laboratory at the University of Arizona (Lot# 80922). Information regarding oocyst isolation and purification can be found elsewhere (http://www.microvet.arizona.edu/research/crypto/cryptoresearch). The oocyst batch was stored in an Antibiotic/Saline/0.01% Tween 20 solution (in the dark at 4 °C). Before use, oocysts were centrifuged twice at 13,400 × *g* for 2 min initially with deionized water (DI) (5415D, Eppendorf, Brinkmann Instrument, Westbury, NY), followed by the selected electrolyte. Prior to transport experiments, oocysts were diluted to the desired concentration (2×10^6 oocysts/mL) in the solution chemistry of interest. Sodium chloride, NaCl (Certified A.C.S. crystal, Fisher Scientific, Fair Lawn, NJ), was chosen as the background electrolyte. The pH of solution was unadjusted (5.6–5.8) for all experiments and the pH change in oocyst suspension was minimal.

2.2. Oocyst characterization

The size and shape of the oocysts were examined from images of the oocysts taken with an inverted microscope in phase contrast mode (Leica Microsystems Inc., Bannockburn, IL).

The lengths and the widths of the oocysts were measured ($n \geq 50$) using an image analysis software (Image J, NIH), and the equivalent radii and aspect ratios of the oocysts were calculated. The average effective diameter was approximately 4.3 μm and the shape of the oocysts was almost spherical (aspect ratio ~1).

The zeta potential of the oocysts was determined at 25 °C as a function of IS (0.1–100 mM) using a ZetaPALS analyzer (Brookhaven Instruments Corporation, Holtsville, NY). The analyzer measured electrophoretic mobility of oocysts and converted to zeta potential based upon the Smoluchowski equation. The measurements were conducted in triplicate for each condition. The obtained oocyst zeta potential values were used in the place of oocyst surface potentials to determine the interaction energies between sand and oocysts using the DLVO theory. Surface potentials of quartz and Ottawa sand were obtained from previous studies (Haznedaroglu et al., 2009; Kim et al., 2009a). A value of 6.5×10^{-21} J was used as the Hamaker constant for the quartz–oocyst–water system (Kuznar and Elimelech, 2006).

2.3. Oocyst enumeration

Oocyst samples were concentrated (factor of 10) via centrifugation at 2000 × *g* for 15 min at 4 °C (Allegre™ 25R Centrifuge, Beckman Coulter™). The concentrated sample was then placed in a microvolume cell holder (50 μL volume) and the concentration of oocysts was determined using a UV/vis spectrophotometer (Ultrospec 4000, Pharmacia Biotech Ltd., Cambridge, UK) at 600 nm. All measurements were performed at least in duplicate. This spectroscopic enumeration method was compared with a direct count method using representative samples. The direct count was carried out using a slightly modified method from that reported by Bradford and Schijven (2002). In brief, 0.1 mL of Aqua-glow fluorescein isothiocyanate (FITC) monoclonal antibody (A400FLR-20×, Waterborne, Inc., New Orleans, LA), which was tenfold diluted in buffer (B100-20, Waterborne, Inc.), was added into 1 mL of oocyst suspension to stain the oocysts. The oocyst suspension with the staining agent was gently mixed (Touch-mixer, Fisher Scientific) and incubated (Low Temperature Incubator, Fisher Scientific) in the dark for at least 45 min at 37 °C. After staining, the suspension was washed twice with 1 mL of DI water via centrifugation (2000 × *g* for 15 min) (Allegre™ 25R Centrifuge, Beckman Coulter™). A 10 μL aliquot of the suspension was then placed in a microscope well and air-dried in a laminar flow chamber. The number of oocysts in the microscope well was counted at 100× and/or 400× magnification using a Leica DM IRB epifluorescent microscope (Leica Microsystems Inc., Bannockburn, IL 60015). The oocysts were identified based upon size, shape, fluorescence, and comparison with positive controls. The concentration was determined from the number of oocysts in the microscope well, the stained suspension volume, and the initial volume of the oocyst sample.

2.4. Porous media

Two types of porous medium were utilized as packing materials in this study: ultra-pure quartz sand (Iota® quartz, Unimin Corp., NC), denoted as quartz sand below, and American Society for Testing and Materials 20/30 unground silica sand (U.S. Silica, Ottawa, IL), denoted as Ottawa sand below. The median grain size (d_{50}) of quartz and Ottawa sand were approximately 275 and 710 μm, respectively. In order to avoid the surface charge heterogeneity caused by any residual metal oxide components and organic matter associated with the quartz and Ottawa sand, the sand was cleaned with 12 N hydrochloric acid (Fisher Scientific) twice and kept in acid overnight (Redman et al., 2004). The mixture was then rinsed with DI water until the rinse water pH was equal to that of the DI water. Prior to wet-packing the column the sand was re-hydrated via boiling in DI water for at least 1 h. The gravimetrically measured bed porosity was determined to be ca. 0.46 and 0.33 for quartz and Ottawa media.

2.5. Batch tests

Batch experiments were conducted in triplicate to determine the relative removal efficiency of oocysts in the absence of pore structure at a given IS (Schijven and Hassanizadeh, 2000; Torkzaban et al., 2006). These experiments were conducted using Ottawa sand because it is the less pure SiO_2 of the two sand types (more chemical heterogeneity) and should result in a greater amount of oocyst removal than the quartz. For batch experiments, 5 g of Ottawa sand and 10 mL of the oocyst suspension (1×10^6 oocysts/mL) was placed into 20 mL scintillation tubes with the temperature kept at approximately 25 °C. The experiments were carried out over the IS range of 0.1–100 mM. The suspension and sand were allowed to equilibrate for 4 h by gently rotating the tubes side over side (8 rpm) on a tube shaker (Labquake®, Branstead/Thermolyne, Bubuque, IA). The initial and final concentrations of oocysts in the suspension were determined based upon the method described above. It should be noted that the oocyst reversibility determined by this approach is operationally defined and may vary with the amount of non-quantified energy imparted to the system. However, the batch results still provide valuable information on the relative capacity of oocyst removal at different IS in the absence of pore structure.

2.6. Column experiments

An adjustable chromatography column (Omnifit, Boonton, NJ) with a 1.5 cm inner diameter and a length of 10 cm was used for transport experiments. Two superficial (Darcy) velocities were employed in this study: 0.2 and 0.5 cm/min. Before initiating the transport experiments more than 10 pore volumes (PV) of DI water was pumped into the column by a peristaltic pump (Cole-Parmer Instrument Company, Vernon Hills, IL), followed by at least 10 PV of the desired electrolyte to equilibrate the inside solution chemistry of the column. A pulse of oocyst suspension at a concentration of 2×10^6 oocysts/mL was then injected into the column for ca. 2.8 PV, followed by an oocyst-free electrolyte solution until the absorbance value was close to background levels. Effluent samples were collected using a fraction collector (RTRV II, Isco Inc, Lincoln, NE) and the concentration of oocysts was spectroscopically determined at a wavelength of 600 nm as described above (Ultrospec 4000, Pharmacia Biotech (Biochrom) Ltd.). In order to prevent oocysts from aggregating, the oocyst suspension was mixed during injection (Automixer, Fisher

Scientific). The degree of aggregation was evaluated by measuring the optical density of the influent oocyst suspension at 600 nm before and after the injection to the column. The deviation was less than 3%, indicating that the aggregation of oocysts in the suspension was minimal during the column experiments. The experiments were conducted at room temperature (25 °C).

The oocyst retention profile (RP) in the column, which describes the distribution of retained oocysts along the length of the column, was obtained after recovery of the breakthrough curve (BTC). The profile for oocysts that were reversibly retained in the column was obtained following a previously reported protocol (Bradford et al., 2006; Kim et al., 2009a). Briefly, the quartz/Ottawa sand was carefully excavated in 1 cm intervals and placed into 50 mL tubes (Fisher Scientific) containing approximately 4 mL of electrolyte (same IS as the during the column experiment). Water was held within the sand during the dissection process by capillary forces. The sand and electrolyte filled tubes were gently shaken, and the concentration of reversibly retained oocysts in the excess electrolyte was determined using the spectroscopic method described above. To determine the volume of the liquid and the mass of sand in each tube, the tubes of sand were dried at 130 °C in an oven (Model 40, GC Lab oven, VWR, Batavia, IL) overnight. The total percentage (M_{total}) of recovered oocysts was calculated as $M_{eff} + M_{DI} + M_{FI} + M_{sand}$. Here M_{eff}, M_{DI}, and M_{FI} denote the percentage of injected oocysts that were collected from the BTC during the initial oocyst transport phase, the DI water flush, and the flow interruption, respectively. The parameter M_{sand} represents the percentage of injected oocysts recovered from column dissection. The validity of this approach was confirmed by the mass balance results (ca. 75–112%).

2.7. Micromodel experiments

In order to better understand the retention mechanism of oocysts under an unfavorable condition, a representative transport experiment was conducted in a specially designed micromodel packed with quartz sand. Detailed information regarding the micromodel experimental protocol can be found elsewhere (Bradford et al., 2006; Kim et al., 2009a). Briefly, the micromodel consists of a glass chamber with an inside dimension of 0.2 cm (D) × 2.0 cm (W) × 7.0 cm (L). Both ends of the chamber were connected to glass tubes of 0.5 cm inside diameter at an angle of about 45°. The quartz sand used in micromodel experiments was wet-packed. Stainless steel needles covered with a stainless steel mesh sheet (150 μm mesh size, McMaster-Carr Co., Aurora, OH), rubber stoppers, and Teflon tubing were used to connect the inlet and outlet sides of the chamber to a syringe pump (KD Scientific Inc.) and a waste bottle, respectively. The oocysts suspension was injected to the chamber at Darcy velocity of 0.2 cm/min for about 3 PV, followed by electrolyte flushing for an additional 5 PV. In order to examine the oocysts retained in the quartz sand, the retained oocysts were stained by the following procedure. Oocyst-free electrolyte, which included Aqua-glow FITC monoclonal antibody (volume ratio of electrolyte to Aqua-glow = 20:1), was flushed to the micromodel chamber. The initial temperature of the electrolyte was 37 °C and the flush duration was approximately 45 min in the dark. After this procedure, oocyst-free electrolyte without antibody was again flushed to the system for an additional 3 PV. The retained oocysts were microscopically examined using a Leica DM IRB epifluorescent microscope (Leica Microsystems Inc., Bannockburn, IL 60015) which had a fluorescent filter set with an excitation wave length of 480 nm and an emission wavelength of 510 nm (maximum magnification of 600×). Images were captured using the microscope connected to a video monitor, a videocassette recorder, and computer system under various intensities of both UV and visible light.

3. Results and discussion

3.1. *Electrokinetic properties of* Cryptosporidium parvum *oocysts and DLVO interaction energy calculations*

Table 1 presents the measured zeta potential of *Cryptosporidium parvum* oocysts as a function of IS. The zeta potential of oocysts became less negative with increasing IS due to compression of the electrical double layer (Elimelech et al., 1995), and became nearly neural when the IS ≥ 1 mM. The DLVO interaction energy between oocysts and sand surfaces was calculated as a function of IS using these zeta potential values and the results for the height of the primary energy barrier, depth of and separation distance at the secondary energy minima are presented in Table 1. At IS = 0.1 mM an insurmountable energy barrier to attachment in the primary minimum was predicted between the oocysts and the two types of surfaces (i.e., 1414 and 1080 kT for quartz and Ottawa sands, respectively). Calculations indicated a significant energy barrier (i.e., 120 kT) and a shallow secondary energy minimum (i.e., 0.282 kT) for oocysts and quartz at IS = 1 mM. In contrast, no energy barrier was predicted between oocysts on quartz or Ottawa sand at IS = 100 mM.

3.2. *Batch test results*

The average oocyst removal efficiency was determined to be 17.2 ± 7.1, 44.5 ± 4.8, 32.3 ± 2.2, and 24.5 ± 4.8% at IS of 0.1, 1, 10, and 100 mM, respectively, for the Ottawa sand. The removal of oocysts under the condition of IS = 0.1 mM may be due to the surface charge heterogeneity of oocysts (Tufenkji et al., 2004; Tufenkji and Elimelech, 2005b). This possibility will be further discussed in Section 3.4.1. Interestingly, the maximum removal of oocysts occurred when the IS = 1 mM, and the removal efficiency decreased with IS. Similar behavior was reported by Kim et al. (2009b) for batch tests using *Escherichia coli* O157:H7, and this trend was attributed to electrosteric repulsion due to the presence of macromolecules. Fig. S1 shows a schematic illustration which compares the total interaction energy with and without the presence of repulsive steric interaction (V_{STERIC}). Based upon the conceptual model, the observed discrepancy with IS from the batch tests may be attributed to V_{STERIC} resulting from macromolecules on the oocyst surface which hinder oocyst attachment in the primary minimum. Specifically, the approach of oocysts to solid surfaces causes the macromolecule layers to be compressed, leading to the subsequent squeeze-out of solvents in the layers and consequently the repulsive

Table 1 – Zeta potentials of oocysts and quartz/Ottawa sand as well as the DLVO interaction energy calculations[a] as a function of IS.

Ionic strength (mM)	Zeta potential (mV)[b]			Depth of secondary minimum[e] (kT)	Separation distance to secondary minimum well (nm)	Energy barrier (kT)
	Oocysts	Quartz[c]	Ottawa[d]			
0.1	−19.8	−68.2		0	NA	1414
			−26.0	0	NA	1080
1	−5.9	−51.6		0.282	92	120
100	−6.6	−13.1		NA[f]	NA	NB[g]
			−1.81	NA	NA	NB

a Including Born-repulsive energy.
b Values measured at unadjusted pH (5.6–5.8) and 25 °C.
c Values adapted from Kim et al. (2009a).
d Values adapted from Haznedaroglu et al. (2009).
e Values calculated within the separation distance of 250 nm.
f Not applicable.
g No energy barrier.

interaction force (V_{STERIC}) between the two surfaces (Israelachivili, 1992; Hiemenz and Rajagopalan, 1997). This effect is unaccounted for in the DLVO calculations ($V_{vdW} + V_{EDL}$). Several studies have previously reported that surface macromolecules, which are present on the surface of oocysts, can give rise to electrosteric repulsion between oocysts and surfaces (Kuznar and Elimelech, 2005, 2006; Liu et al., 2009).

3.3. *Observed transport and retention behavior of oocysts*

Oocyst transport and retention was investigated as a function of IS (0.1, 1, and 100 mM), Darcy velocity ($q = 0.2$ and 0.5 cm/min), and grain size ($d_{50} = 275$ and 710 μm) in the packed-bed column. Each of these topics will be discussed separately below. Fig. 1 presents oocyst BTCs in quartz (Figs. 1a,b) and Ottawa sand (Fig. 1c) as a function of IS and q. Relevant system parameters are provided in the figure caption. In this figure the relative effluent concentrations (C/C_o) are plotted as function of PV. The corresponding oocyst RPs are shown in Figs. 2a–c. In this case, the normalized concentration of oocysts that were retained in the sand ($N_o N_{to}^{-1}$ g^{-1} sand; where N_o and N_{to} are the number of retained oocysts and the total number of injected oocysts, respectively) are plotted as a function of dimensionless distance from the column inlet. Relatively good mass balance was achieved in these experiments (ca. 75–113%) and this information is summarized in Table 2. The replicate test result for quartz sand (IS = 1 mM and $q = 0.2$ cm/min) is also presented in Table 2.

Figs. 1a–c indicate that increasing the IS led to more oocyst retention in the quartz and Ottawa sands. A similar retention trend with IS was observed at both $q = 0.2$ (Figs. 1a,c) and 0.5 (Figs. 1b,c) cm/min. The RPs shown in Figs. 2a,b are consistent with information presented in the BTCs, in that increasing the IS produced more oocyst retention. This behavior is qualitatively consistent with DLVO predictions of a decreasing energy barrier to oocyst interaction with the sand with increasing IS (Table 1).

The influence of velocity on oocyst transport in the column packed with quartz sand can be deduced by comparing Figs. 1a ($q = 0.2$ cm/min) and b ($q = 0.5$ cm/min) at a given IS. Similar information is available for the Ottawa sand in Fig. 1c. Greater oocyst transport occurred at the higher velocity condition under which DLVO predictions indicated a significant energy barrier to primary minimum interaction existing and little or no secondary energy minimum (unfavorable conditions). Specifically, at IS = 0.1 mM for q of 0.2 and 0.5 cm/min, the value of M_{eff} was 50.6 and 68.7% in quartz sand and 75.8 and 96.3% in Ottawa sand, respectively (Table 2). Similarly, in quartz sand at IS = 1 mM the value of M_{eff} was 26.2 and 40.0% for q of 0.2 and 0.5 cm/min, respectively. No significant change was observed in the shape of RPs (Fig. 2) with changing velocity under these conditions. The effect of velocity on oocyst transport and retention was more complicated when the IS = 100 mM. This information will be discussed in detail in Section 3.4.3.

Fig. 1c shows oocyst BTCs as a function of IS (0.1 and 100 mM) and q (0.2 and 0.5 cm/min) when the column was packed with Ottawa sand ($d_{50} = 710$ μm). Comparison of Figs. 1c with a and b under similar IS and q conditions demonstrates the influence of grain size on oocyst transport and retention behavior. Overall, oocysts were transported in the column packed with Ottawa sand ($d_{50} = 710$ μm) to a greater extend than in quartz sand ($d_{50} = 275$ μm) at a given IS and velocity condition. Specifically, at IS = 0.1 mM and 0.2 cm/min the value of M_{eff} was 75.8% in Ottawa sand and 50.6% in quartz sand. When the IS = 100 mM and $q = 0.2$ cm/min the value of M_{eff} was 14.6% in Ottawa sand and 1.1% in quartz sand. Similar trends were observed for the BTCs obtained at $q = 0.5$ cm/min, but in this case the effect of grain size on oocyst transport was more pronounced. Specifically, at IS = 0.1 mM and $q = 0.5$ cm/min the value of M_{eff} was 96.3% in Ottawa sand and 68.7% in quartz sand. When the IS = 100 mM and $q = 0.5$ cm/min the value of M_{eff} was 50.9% in Ottawa sand and 1.0% in quartz sand.

3.4. *Oocyst retention mechanisms*

The experimental results discussed above indicate that the oocyst transport and retention behavior is very sensitive to IS, velocity, and grain size. Below we discuss the critical roles of low velocity regions, weak attractive interactions, and steric

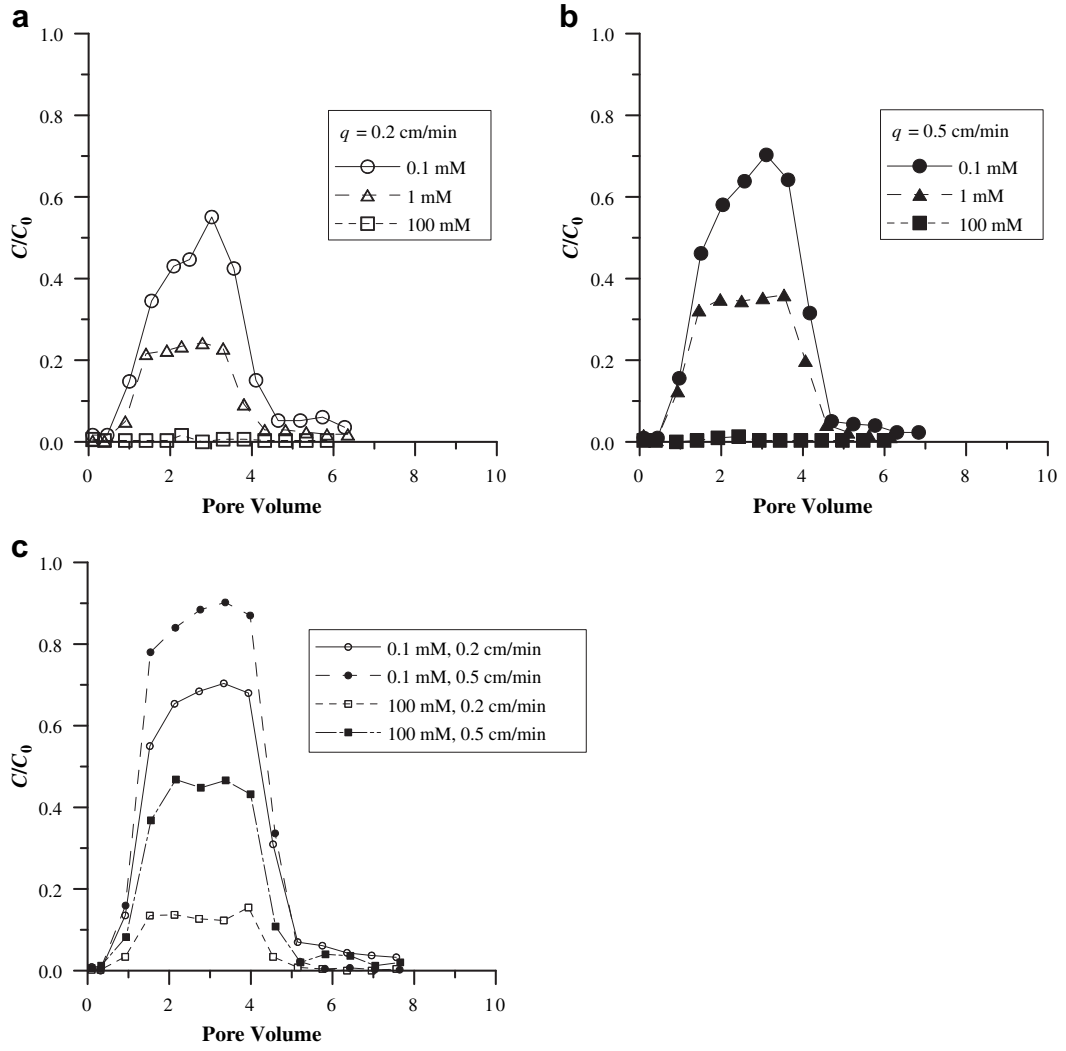

Fig. 1 – Oocyst breakthrough curves (BTCs) as a function of IS (0.1, 1, and 100 mM) at Darcy velocity (*q*) of (a) 0.2 cm/min and (b) 0.5 cm/min in the column packed with quartz sand (d_{50} = 275 μm). (c) Oocyst BTCs as a function of IS (0.1 and 100 mM) and *q* (0.2 and 0.5 cm/min) in the column packed with Ottawa sand (d_{50} = 710 μm).

repulsion on oocyst retention. The relative importance of each of these retention factors is demonstrated to depend on the solution IS.

3.4.1. *IS = 0.1 mM*

Recent literature has demonstrated that low velocity regions in porous media are very important for the retention of colloids and biocolloids under unfavorable condition (e.g., Bradford et al., 2006; Li et al., 2006; Torkzaban et al., 2008; Bradford et al., 2009). These low velocity regions occur as a result of pore structure near grain–grain contacts, in small pore spaces, and adjacent to surface roughness, and may also be associated with flow vortices (Torkzaban et al., 2008). Torque balance calculations indicate that such regions are hydrodynamically favorable for retention (Torkzaban et al., 2007, 2008), and our experimental results support this concept. In particular, batch test results and DLVO calculations demonstrated that conditions were highly unfavorable for oocyst retention at IS = 0.1 mM. Nevertheless, Fig. 1 and Table 2 indicate that significant amounts of oocyst retention occurred under these conditions (3.7–49.4%), and that the oocyst retention increased with decreasing *q* and d_{50}.

Fig. 3 shows illustrative micromodel images of the final oocyst retention in the quartz sand when the IS = 0.1 mM and *q* = 0.2 cm/min. The images demonstrate that the majority of oocysts were retained in low velocity regions. In addition, the reversibility of oocysts from the column experiments under this condition further supports this hypothesis (M_{total} = 84.9–112.2%). The results at IS = 0.1 mM confirmed our DLVO calculations that indicated little potential for primary minimum attachment of oocysts on sands under these conditions, and indicates that charge heterogeneity likely played only a minor role in oocyst retention under this condition.

An interesting finding from the column study is the decrease in oocyst retention observed with increased velocity under this otherwise "unfavorable" condition. Specifically, a higher *q* (0.5 versus 0.2 cm/min) led to less oocyst retention in the column, indicating that the oocyst retention in low

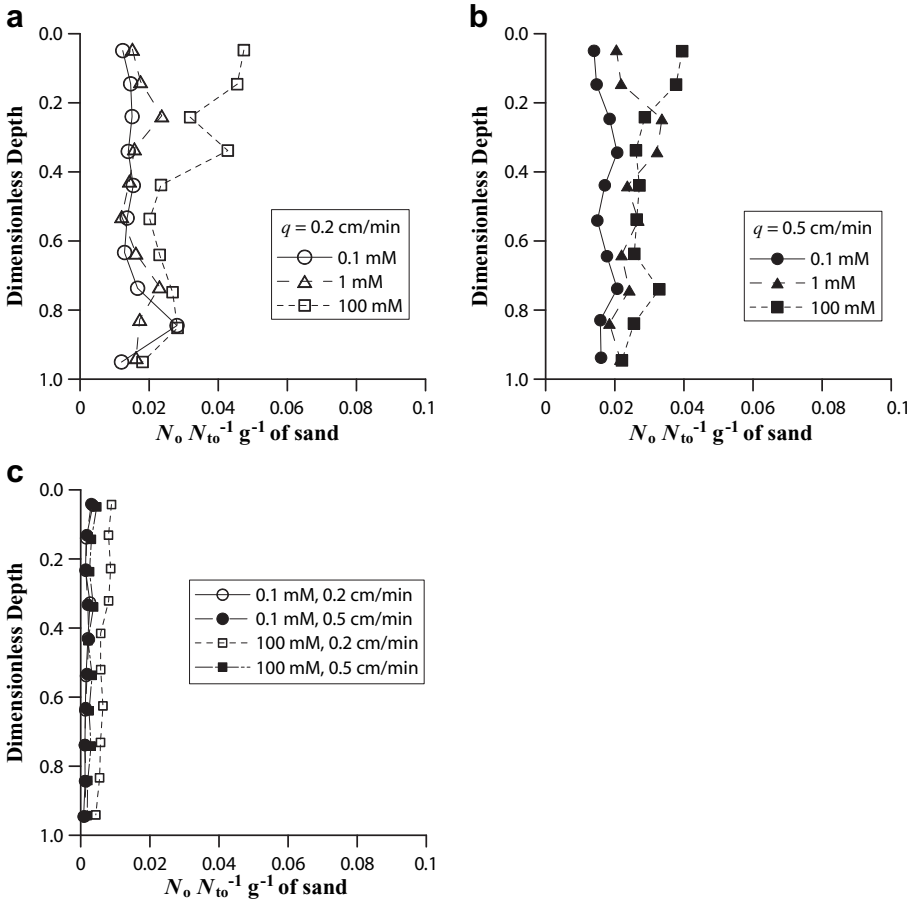

Fig. 2 – Oocyst retention profiles (RPs) as a function of IS (0.1, 1, and 100 mM) at Darcy velocity (q) of (a) 0.2 cm/min and (b) 0.5 cm/min in the column packed with quartz sand (d_{50} = 275 μm). (c) Oocyst RPs as a function of IS (0.1 and 100 mM) and q (0.2 and 0.5 cm/min) in the column packed with Ottawa sand (d_{50} = 710 μm). Note that the RP for the IS = 1 mM condition in (a) was obtained after DI flush and flow interruption tests. The X-axis represents the normalized concentration of the oocysts (the number of oocysts in each section of column, N_o, divided by the total number injected into the column, N_{to}) per gram of dry sand.

Table 2 – Mass balance results for oocysts obtained from column experiments.

Grain type	Darcy velocity (cm/min)	Ionic strength (mM)	η[a]	M_{eff} (%)	M_{CFT} (%)[b]	M_{DI} (%)	M_{FI} (%)	M_{sand} (%)	M_{total} (%)
Quartz (d_{50} = 275 μm)	0.2	0.1	1.9×10^{-2}	50.6				39.5	87.8
		1		26.2		16.8	26.3	42.9	112.2
				19.4				72.2	91.6
		100		1.1	0.3			77.4	78.5
	0.5	0.1	1.1×10^{-2}	68.7				43.5	112.2
		1		40.0				61.9	101.9
		100		1.0	4.0			73.7	74.7
Ottawa (d_{50} = 710 μm)	0.2	0.1	1.5×10^{-2}	75.8		3.4	0.5	5.2	84.9
		100		14.6	11.6	37.1	13.0	20.1	84.8
	0.5	0.1	6.9×10^{-3}	96.3		1.6	0.2	5.3	103.4
		100		50.9	37.7	23.3	12.7	8.8	95.7

M_{eff}, M_{FI}, M_{DI}, and M_{sand} represent the amount of the oocysts recovered from the initial oocyst transport phase, flow interruption, DI flush, and column dissection. M_{eff}, M_{FI}, and M_{DI} were determined by integrating beneath the corresponding effluent concentration profile in Figs. 1 and 4. M_{sand} was determined from the experimentally determined retention profile in Fig. 2. M_{total} represents the sum of all percentages (i.e., M_{eff}, M_{FI}, M_{DI}, and M_{sand}).

a Single collector contact efficiency calculated from TE model (Tufenkji and Elimelech, 2004).

b Predicted breakthrough values based upon the classic filtration theory (Yao et al., 1971).

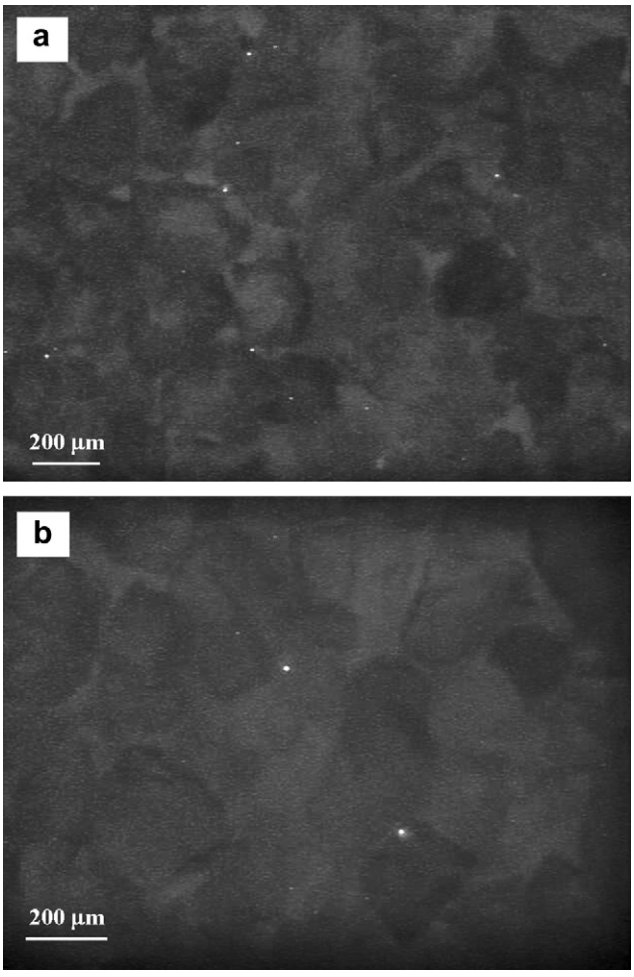

Fig. 3 – Images of oocysts retained in quartz sand. The experiments were carried out at IS = 0.1 mM and Darcy velocity of 0.2 cm/min. White dots denote the oocysts retained in the column. The images were taken at two different locations.

velocity regions was also dependent on the Darcy velocity. Bradford et al. (2009) recently discussed how a "dual permeability model" may be used to investigate enhanced colloid retention in such low velocity regions. This study demonstrated that mass transfer between high and low velocity regions (A and B regions in Fig. S2, respectively) within the pore space and the relative differences in velocities within these regions are critical factors that affect colloid retention under unfavorable conditions. The dual permeability model results they reported are consistent with our observations in that increasing q led to a decrease in oocyst retention in either sand under unfavorable (IS = 0.1 mM) conditions (Fig. 1).

3.4.2. *IS = 1 mM*

At IS = 1 mM, DLVO calculations suggest a shallow secondary energy minimum occurred between the oocysts and the quartz sand. However, one could argue the secondary well was not deep enough for oocysts to attach onto the quartz surface (ca. 0.3 kT). These DLVO calculations were based on measured values of zeta potential for oocysts and sand that implicitly neglects nanoscale chemical heterogeneity and surface roughness (considers only mean properties). Kozlova and Santore (2006) reported that nanoscale chemical heterogeneity may enhance the adhesive interaction between two surfaces, especially at a higher IS (Duffadar and Davis, 2008). Hoek et al. (2003) showed that the presence of surface roughness could reduce or enhance adhesive interactions between two surfaces depending on the roughness and the colloid size. The sand grains and oocysts used in this study are known to have rough surfaces (Considine et al., 2001, 2002; Tufenkji et al., 2004). Hence, the above information indicates that weak attractive interactions may occur at IS = 1 mM due to a combination of secondary energy minimum, nanoscale chemical heterogeneity, and surface roughness.

In order to better examine the contribution of weak attractive interactions to oocyst retention, an additional experiment was conducted. Specifically, after recovery of the BTC in the quartz sand when the IS = 1 mM and q = 0.2 cm/min, DI water was flushed through the column followed by a flow interruption of 12 h, and subsequently DI water, all at the same rate (q = 0.2 cm/min). Fig. 4a and Table 2 show the results of the DI flush and flow interruption. By switching to DI water, those oocysts retained by weak attractive interactions at IS = 1 mM should be released, and indeed this step resulted in approximately 16.8% of the oocysts eluting. In addition, flow interruption results indicated that 26.3% of the total oocysts were released from the column and M_{sand} = 42.9%. These results demonstrate the importance of low velocity regions for oocyst retention in the column when the IS was 1 mM. Mass balance results at low and high velocity conditions (i.e., $M_{FI} + M_{sand}$ = 69.2 and 61.9% at q of 0.2 and 0.5 cm/min, respectively) also support this hypothesis.

3.4.3. *IS = 100 mM*

DLVO calculations presented in Table 1 indicate that the interaction condition between oocysts and sand surfaces is favorable at IS = 100 mM. Conversely, results from batch experiments indicate that oocysts retention decreased with increasing IS and that only a relatively small fraction of the oocysts were retained at IS = 100 mM (ca. 24.5 ± 4.8%). These observations were attributed to reversible oocyst–sand interaction due to steric repulsion of oocyst surface macromolecules (Kuznar and Elimelech, 2006; Liu et al., 2009). Additional evidence for and implications of steric repulsion of oocysts in the column experiments will be provided below.

CFT theory is commonly employed to predict colloid transport in porous media under favorable attachment conditions (e.g., IS = 100 mM). Predicted values of the collector efficiency (η) from CFT (Tufenkji and Elimelech, 2004) are provided in Table 2. CFT predicts that increasing velocity and d_{50} will produce a lower value of η and less oocyst retention. No apparent velocity dependence was observed in the oocyst BTCs for quartz sand at IS = 100 mM (Figs. 1a,b). The observed oocyst breakthroughs are similar with the predicted values from the CFT (M_{eff} = 1.1% and M_{CFT} = 0.3% at q = 0.2 cm/min, and M_{eff} = 1.0% and M_{CFT} = 4.0% at q = 0.5 cm/min in Table 2). However, the experimentally determined oocyst RPs show a deviation from the exponential prediction of CFT (goodness of fitting, r^2 = 0.674 and 0.664 for q of 0.2 and 0.5 cm/min, respectively). This observation indicates that other mechanisms, which classic theories (CFT and DLVO theories) do not

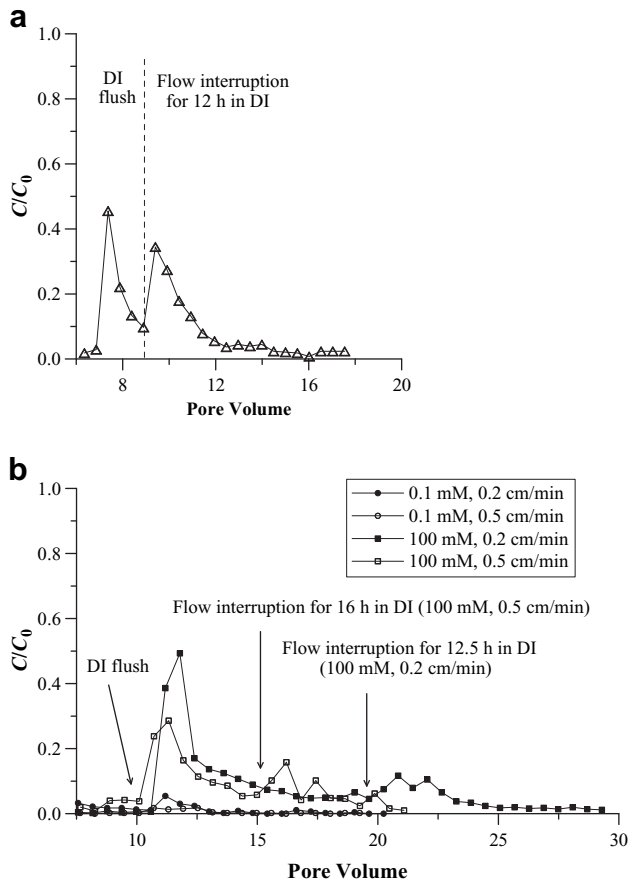

Fig. 4 – Oocyst elution curves by DI flush and flow interruption. The experimental conditions are as follows: (a) Darcy velocity (q) of 0.2 cm/min, IS = 1 mM, grain type/size = quartz/275 μm; (b) q = 0.2 and 0.5 cm/min, IS = 0.1 and 100 mM, grain type/size = Ottawa/710 μm. Note that the starting position of DI flush and flow interruption for IS = 0.1 mM conditions were not indicated in (b) since the released amount was negligible.

account for, are likely involved in oocyst retention. In contrast, a velocity dependence was observed in the BTC results for the Ottawa sand at IS = 100 mM (when q was 0.2 and 0.5 cm/min the value of M_{eff} was 14.6 and 50.9%, respectively). Hence, the observed velocity effect at IS = 100 mM was apparently coupled with the grain size. Further comparison of BTCs with the CFT prediction suggests that the experimentally observed oocyst breakthroughs at two velocity conditions were greater than the predicted values (M_{eff} = 14.6% and M_{CFT} = 11.6% at q = 0.2 cm/min, and M_{eff} = 50.9% and M_{CFT} = 37.7% at q = 0.5 cm/min in Table 2). The difference between experimentally determined and predicted values was more pronounced at the higher velocity. Furthermore, the column mass balance information indicated that the oocysts were reversibly retained (74.7–95.7% total recovery). All of these factors support our hypothesis that weak interactions occurred under these conditions as a result of steric repulsion of oocyst surface macromolecules.

In order to further test this hypothesis, experiments were carried out as follows: after recovery of the BTCs (IS = 100 mM), additional DI water flushing and flow interruption (≥ 12 h) experiments were carried out in Ottawa sand at two different velocities (q = 0.2 and 0.5 cm/min) (Fig. 4b). The results clearly indicated that a weak attractive interaction existed between the Ottawa sand and oocysts, and this interaction was sensitive to changing IS and velocity (37.1 and 23.3% oocyst elution during DI flush when q = 0.2 and 0.5 cm/min, respectively). DLVO calculations indicate that this weak interaction is unlikely due to a secondary energy minimum interaction. Rather, steric repulsion appears to be the more logical explanation of the weak interaction under favorable (DLVO) conditions. The flow interruption (13.0 and 12.7% oocyst release from the column for low and high velocity, respectively) and M_{sand} (20.1 and 8.8% oocyst recovery at low and high velocity, respectively) results (Table 2) indicate a reversible interaction that is also associated with low velocity regions. This trend, the discrepancy between the observed oocyst transport and the theoretical prediction in Ottawa sand at IS = 100 mM (Fig. 1c and Table 2), and the relatively uniform distribution of the RPs with column depth at IS = 100 mM for quartz sand (Figs. 2a,b) may be attributed to differences in mass transfer and torque balance between low and high velocity regions (Fig. S2) as described in earlier sections. In particular, oocysts that are weakly associated with sand by steric repulsion may slowly translate along with the sand surface to lower velocity regions that are hydrodynamically favorable for retention or detach from the surface due to the hydrodynamic drag force (Bradford et al., 2007; Kuznar and Elimelech, 2007; Torkzaban et al., 2007, 2008). In fact, the mass balance information for Ottawa sand (Table 2) indicates that a significant amount of oocysts were retained in the low velocity regions ($M_{FI} + M_{sand}$ = 33.1 and 21.5% for 0.2 and 0.5 cm/min, respectively).

4. Conclusions

The coupled role of solution IS, Darcy velocity, and grain size on oocyst transport and retention was investigated in saturated packed-bed column. The results showed that oocyst retention is a complex process that is very sensitive to solution IS, velocity, and grain size. Two important findings were obtained from this study. First, the extent of oocyst retention in saturated porous media varied with velocity under unfavorable conditions. Specifically, the oocyst retention increased with decreasing velocity due to increasing mass transfer from the liquid to the solid phase or from high to low velocity regions. Another notable observation was reversible retention of oocysts under conditions, which DLVO theory predicts to be favorable for irreversible attachment of oocysts to sand surfaces. These trends were attributed to weak interactions of oocysts to the sand surface by steric repulsion due to the presence of oocyst surface macromolecules. Findings from this study demonstrate the potential limitations of classic theories (CFT and DLVO theories) in quantifying the transport and retention mechanisms of oocysts. Furthermore, caution is warranted when estimating the travel distance of oocysts in soil and aquifer environments under chemically favorable conditions.

Acknowledgements

This research was funded by the Manure and Byproduct Utilization Project of the USDA-ARS (NP 206), and by a grant from the USDA CSREES NRI (NRI 2006-02541). Mention of trade names and company names in this manuscript does not imply any endorsement or preferential treatment by the USDA.

Appendix A. Supplemental material

Supplementary information for this manuscript can be downloaded at doi:10.1016/j.watres.2009.09.041.

REFERENCES

Bitton, G. (2005) Wastewater Microbiology, John Wiley & Sons, Hoboken, N.J.

Bradford, S.A., Bettahar, M., 2005. Straining, attachment, and detachment of *Cryptosporidium* oocysts in saturated porous media. J. Environ. Qual 34 (2), 469–480.

Bradford, S.A., Schijven, J., 2002. Release of *Cryptosporidium* and *Giardia* from dairy calf manure: impact of solution salinity. Environ. Sci. Technol 36 (18), 3916–3923.

Bradford, S.A., Yates, S.R., Bettahar, M., Simunek, J., 2002. Physical factors affecting the transport and fate of colloids in saturated porous media. Water Resour. Res. 38 (12), 1327. 1310.1029/2002WR001340.

Bradford, S.A., Simunek, J., Walker, S.L., 2006. Transport and straining of *E. coli O157:H7* in saturated porous media. Water Resour. Res 42, W12S12. doi:10.1029/2005WR004805.

Bradford, S.A., Torkzaban, S., Walker, S.L., 2007. Coupling of physical and chemical mechanisms of colloid straining in saturated porous media. Water Res. 41, 3012–3024.

Bradford, S.A., Torkzaban, S., Leij, F., Simunek, J., van Genuchten, M.T., 2009. Modeling the coupled effects of pore space geometry and velocity on colloid transport and retention. Water Resour. Res 45, W02414. 02410.01029/02008WR007096.

Brush, C.F., Walter, M.F., Anguish, L.J., Ghiorse, W.C., 1998. Influence of pretreatment and experimental conditions on electrophoretic mobility and hydrophobicity of *Cryptosporidium parvum* oocysts. Appl. Environ. Microbiol. 64 (11), 4439–4445.

Byrd, T.L., Walz, J.Y., 2007. Investigation of the interaction force between *Cryptosporidium parvum* oocysts and solid surfaces. Langmuir 23 (14), 7475–7483.

Centers for Disease Control and Prevention, 1997. Cryptosporidium and Water: A Public Health Handbook. Georgia: Working Group on Waterborne Cryptosporidiosis, Atlanta.

Considine, R.F., Drummond, C.J., Dixon, D.R., 2001. Force of interaction between a biocolloid and an inorganic oxide: complexity of surface deformation, roughness, and brushlike behavior. Langmuir 17 (20), 6325–6335.

Considine, R.F., Dixon, D.R., Drummond, C.J., 2002. Oocysts of *Cryptosporidium parvum* and model sand surfaces in aqueous solutions: an atomic force microscope (AFM) study. Water Res. 36, 3421–3428.

Cortis, A., Harter, T., Hou, L., Atwill, E.R., Packman, A.I., Green, P.G., 2006. Transport of *Cryptosporidium parvum* in porous media: long-term elution experiments and continuous time random walk filtration modeling. Water Resour. Res 42, W12S13. doi:10.1029/2006WR004897.

Darnault, C.J.G., Steenhuis, T.S., Garnier, P., Kim, Y.-J., Jenkins, M.B., Ghiorse, W.C., Baveye, P.C., Parlange, J.-Y., 2004. Preferential flow and transport of *Cryptosporidium parvum* oocysts through the vadose zone: experiments and modeling. Vadose Zone J 3, 262–270.

Derjaguin, B.V., Landau, L.D., 1941. Acta Physicochim. U.S.S.R 14, 300.

Duffadar, R.D., Davis, J.M., 2008. Dynamic adhesion behavior of micrometer-scale particles flowing over patchy surfaces with nanoscale electrostatic heterogeneity. J. Colloid Interface Sci. 326, 18–27.

Elimelech, M., Gregory, J., Jia, X., Williams, R.A., 1995. Particle Deposition and Aggregation: Measurement, Modeling and Simulation. Butterworth-Heinemann, Oxford, England.

Hahn, M.W., O'Melia, C.R., 2004. Deposition and reentrainment of Brownian particles in porous media under unfavorable chemical conditions: some concepts and applications. Environ. Sci. Technol 38 (1), 210–220.

Harris, J.R., Petry, F., 1999. *Cryptosporidium parvum*: structural components of the oocyst wall. J. Parasitol 85 (5), 839–849.

Harter, T., Wagner, S., Atwill, E.R., 2000. Colloid transport and filtration of *Cryptosporidium parvum* in sandy soils and aquifer sediments. Environ. Sci. Technol 34, 62–70.

Haznedaroglu, B.Z., Kim, H.N., Bradford, S.A., Walker, S.L., 2009. Relative transport behavior of *Escherichia coli* O157:H7 and *Salmonella enterica* serovar pullorum in packed bed column systems: influence of solution chemistry and cell concentration. Environ. Sci. Technol 43 (6), 1838–1844.

Hiemenz, P.C., Rajagopalan, R., 1997. Principles of Colloid and Surface Chemistry, third ed. Marcel Dekker, New York.

Hoek, E.M.V., Bhattacharjee, S., Elimelech, M., 2003. Effect of membrane surface roughness on colloid–membrane DLVO interactions. Langmuir 19, 4836–4847.

Hsu, B.-M., Huang, C., Pan, J.R., 2001. Filtration behaviors of *Giardia* and *Cryptosporidium*-ionic strength and pH effects. Water Res. 35 (16), 3777–3782.

Huck, P.M., Coffey, B.M., Emelko, M.B., Maurizio, D.D., Slawson, R. M., Anderson, W.B., Van den Oever, J., 2002. Effects of filter operation on *Cryptosporidium* removal. J. Am. Water Works Assoc. 94 (6), 97–111.

Israelachvili, J.N., 1992. Intermolecular and Surface Forces. Academic Press, Amsterdam, Boston.

Kim, H.N., Bradford, S.A., Walker, S.L., 2009a. *Escherichia coli* O157:H7 transport in saturated porous media: role of solution chemistry and surface macromolecules. Environ. Sci. Technol. 43 (12), 4340–4347.

Kim, H.N., Hong, Y., Lee, I., Bradford, S.A., Walker, S.L., 2009b. Surface characteristics and adhesion behavior of *Escherichia coli* O157:H7: role of extracellular macromolecules. Biomacromolecules 10, 2556–2564.

Kozlova, N., Santore, M.M., 2006. Manipulation of micrometer-scale adhesion by tuning nanometer-scale surface features. Langmuir 22, 1135–1142.

Kuznar, Z.A., Elimelech, M., 2004. Adhesion kinetics of viable *Cryptosporidium parvum* oocysts to quartz surfaces. Environ. Sci. Technol 38 (24), 6839–6845.

Kuznar, Z.A., Elimelech, M., 2005. Role of surface proteins in the deposition kinetics of *Cryptosporidium parvum* oocysts. Langmuir 21 (2), 710–716.

Kuznar, Z.A., Elimelech, M., 2006. *Cryptosporidium* oocyst surface macromolecules significantly hinder oocyst attachment. Environ. Sci. Technol 40 (6), 1837–1842.

Kuznar, Z.A., Elimelech, M., 2007. Direct microscopic observation of particle deposition in porous media: role of the secondary energy minimum. Colloid Surf. A: Physicochem. Eng. Aspects 294, 156–162.

Li, X., Lin, C.-L., Miller, J.D., Johnson, W.P., 2006. Role of grain-to-grain contacts on profiles of retained colloids in porous media in the presence of an energy barrier to deposition. Environ. Sci. Technol 40 (12), 3769–3774.

Liu, Y., Janjaroen, D., Kuhlenschmidt, M.S., Kuhlenschmidt, T.B., Nguyen, T.H., 2009. Deposition of *Cryptosporidium parvum* oocysts on natural organic matter surfaces: microscopic evidence for secondary minimum deposition in a radial stagnation point flow cell. Langmuir 25 (3), 1594–1605.

Redman, J.A., Walker, S.L., Elimelech, M., 2004. Bacterial adhesion and transport in porous media: role of the secondary energy minimum. Environ. Sci. Technol 38 (6), 1777–1785.

Schijven, J.F., Hassanizadeh, S.H., 2000. Removal of viruses by soil passage: overview of modeling, processes, and parameters. Crit. Rev. Environ. Sci. Technol 30 (1), 49–127.

Timms, S., Slade, J.S., Fricker, C.R., 1995. Removal of *Cryptosporidium* by slow sand filtration. Wat. Sci. Tech 31 (5-6), 81–84.

Torkzaban, S., Bradford, S.A., van Genuchten, M.T., Walker, S.L. , 2006. Colloid transport in unsaturated porous media: the role of water content and ionic strength on particle straining. J. Contam. Hydrol 96, 113–127.

Torkzaban, S., Bradford, S.A., Walker, S.L., 2007. Resolving the coupled effects of hydrodynamics and DLVO forces on colloid attachment in porous media. Langmuir 23 (19), 9652–9660.

Torkzaban, S., Tazehkand, S.S., Walker, S.L., Bradford, S.A., 2008. Transport and fate of bacteria in porous media: coupled effects of chemical conditions and pore space geometry. Water Resour. Res 44, W04403. 04410.01029/02007WR006541.

Tufenkji, N., Elimelech, M., 2004. Correlation equation for predicting single-collector efficiency in physicochemical filtration in saturated porous media. Environ. Sci. Technol 38 (2), 529–536.

Tufenkji, N., Elimelech, M., 2005a. Breakdown of colloid filtration theory: role of secondary energy minimum and surface charge heterogeneities. Langmuir 21, 841–852.

Tufenkji, N., Elimelech, M., 2005b. Spatial distribution of *Cryptosporidium* oocysts in porous media: evidence for dual mode deposition. Environ. Sci. Technol 39 (10), 3620–3629.

Tufenkji, N., Ryan, J.N., Elimelech, M., 2002. The promise of bank filtration. Environ. Sci. Technol 36 (21), 422A–428A.

Tufenkji, N., Miller, G.F., Ryan, J.N., Harvey, R.W., Elimelech, M., 2004. Transport of *Cryptosporidium* oocysts in porous media: role of straining and physicochemical filtration. Environ. Sci. Technol 38, 5932–5938.

Tufenkji, N., Dixon, D.R., Considine, R., Drummond, C.J., 2006. Multi-scale *Cryptosporidium*/sand interactions in water treatment. Water Res. 40, 3315–3331.

Verwey, E.J.W., Overbeek, J.T.G. (1948) Theory of the Stability of Lyophobic Colloids Elsevier, Amsterdam.

Yao, K.M., Habibian, M.T., O'Melia, C.R., 1971. Water and waste water filtration: concepts and applications. Environ. Sci. Technol 5 (11), 1105–1112.